

BER Analysis and Optimization of Direct Antenna Modulation for Magnetic Induction Communication

Ryan Chapman, Marlin Prince, and Hongzhi Guo

Norfolk State University

Norfolk, VA, USA

Abstract—The wireless communication range of RF (Radio Frequency) signals in underground environments is limited due to the short skin depth and geometric inhomogeneity. Magnetic induction-based near field communication using long-wavelength signals provides a low-power, low-cost, and long-range solution. Due to the fundamental limitation of antenna bandwidth, the data rate of magnetic induction communication is small, especially using LF or VLF carrier frequencies. Recently, this limitation has been addressed by the use of direct antenna modulation (DAM). Although DAM-based antennas have been widely developed and accepted, it is not clear how to design optimal receivers to build an integrated communication system. In this paper, the bit error rate (BER) of two receiving architectures for magnetic induction communication with DAM using an integrator and a correlator are studied. The demodulation schemes are introduced and analyzed. Analytical models are developed, optimized, and compared.

Index Terms—BER analysis, direct antenna modulation, near field communication, optimal receiver.

I. INTRODUCTION

Wireless underground sensor network plays an important role in precision agriculture and underground pipeline monitoring [1], [2]. The dense and complex underground environment poses significant challenges on the signal propagation, communication, and networking for existing wireless techniques such as Zigbee and cellular networks, which are based on RF (Radio Frequency) signals. Wireless sensor networks in the terrestrial environment cannot be simply used in underground environments due to their high power consumption, large device profile, and high propagation loss.

Magnetic induction-based (MI) near field communication uses long-wavelength signals to reduce the propagation loss in underground environments [3]. By using LF (30–300 kHz) or VLF (3–30 kHz) signals, MI communication can even penetrate through metal walls [4] for underground metallic pipeline monitoring. Wireless underground sensor networks using MI communication have received wide acceptance [5]. MI communication transceivers use high-Q coils to obtain a long communication range. However, due to the fundamental limitation of coil bandwidth, the high-Q coils have very narrow bandwidths [6] [7]. In addition, the carrier frequency of MI communication is also small (usually lower than 30 MHz) and the bandwidth becomes extremely narrow. Thus, according to Shannon channel capacity, the achievable data rate is limited. Many applications such as underground pipeline inspection using in-pipe robots require high-data-rate MI communication

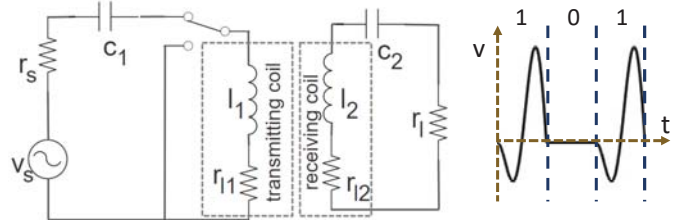


Fig. 1. Equivalent circuit model for DAM.

Fig. 2. An example of received signals.

to send sensing data and provide navigation support. Therefore, it is desirable to develop high-speed MI communication based on low carrier frequencies. This problem is fundamentally different from traditional RF communications where the bandwidth of baseband signals is much smaller than the carrier frequency. For MI communication, the carrier frequency is so small which may not allow wide baseband signal modulation.

Direct antenna modulation (DAM) for MI communication was proposed in [6], [7]. The data transmission is no longer limited by the coil bandwidth. By using a switch the transmitted signals can be modulated directly on a coil using On-Off modulation. It has significant potentials to realize fast MI communication using low carrier frequencies. For example, by using 13.56 MHz as the carrier frequency, one can obtain a 13.56 Mbps data rate ideally. In [6], [7], the modulation and communication circuits are designed and analyzed. In this paper, we focus on the receiver side and develop optimal receivers using an integrator and a correlator. We develop analytical bit error rate (BER) models to evaluate the performance of the receiving architectures. Then, we analyze and optimize the receivers and compare their performance.

II. BER MODELS FOR DIRECT ANTENNA MODULATION

In this section, we review the DAM for MI communication. Then, we develop the analytical BER models for optimal receivers and optimize their performance.

A. Direct Antenna Modulation

The DAM is controlled by a switch, as shown in Fig. 1, where v_s is the source, r_s is the source resistance, c_1 and c_2 are capacitors, l_1 and l_2 are self-inductance, r_{l1} and r_{l2} are coil resistances, and r_l is the load resistance. When a bit “1” is transmitted, the switch turns to the capacitor to form a traditional RLC circuit. When a bit “0” is transmitted, the switch turns to the ground and the current in the circuit decreases. By switching at the maximum current moment,

Corresponding author Hongzhi Guo. Email hguo@nsu.edu. Phone: +1 757-823-2309

when a bit “1” is transmitted the induced voltage on the receiving coil’s load can be written as

$$v_{r1}(t) = -r_l c_1 \left[c_2 + (i_{sw} - c_2) e^{-\frac{\omega_0 t}{2Q_t}} \right] \sin(\omega_0 t), \quad (1)$$

where i_{sw} is the current at the switching moment, $\omega_0 = 2\pi f_0 = 2\pi/T_0$, f_0 is the carrier frequency, $Q_t = \omega_0 l_1 / (r_s + r_{l1})$, $c_1 = \frac{\omega_0 m}{r_l + r_{l2}}$ and $c_2 = \frac{v_0}{r_s + r_{l1}}$, while when a bit “0” is transmitted, the induced voltage on the receiving coil’s load is

$$v_{r0}(t) = \frac{r_l c_1 i_{sw}}{\alpha Q_t} e^{-\frac{\omega_0 t}{\alpha Q_t}}, \quad (2)$$

where $\alpha = (r_{l1} + r_s)/r_{l1}$. The complete derivations of the induced currents are given in [6]. An example of the received voltage signal across a resistive load is shown in Fig. 2. In traditional RLC circuits, when the circuit has a large Q_t , $v_{r0}(t) \approx v_{r1}(t)$ and the receiver cannot successfully demodulate the transmitted data. For DAM, the induced voltage in the receiver for bit “1” and bit “0” are clearly different, which is desirable for efficient detection.

In this paper, we propose two optimal receivers using an integrator and a correlator, as shown in Fig. 3. For the integration-based solution, we use a full-wave bridge rectifier to obtain positive voltages and sample the output every T_0 , which is compared with a threshold value to detect the transmitted data. When a bit “0” is transmitted the induced current in a receiver is almost zero, while by using the integration-based receiver we can obtain a relatively large value when a bit “1” is transmitted. Such a large difference can be used to distinguish the bit “0” and bit “1”. For the correlation-based solution, the received signal is correlated with a predefined signal. If a bit “1” is transmitted, the output is larger than that when a bit “0” is transmitted. Next, we derive analytical BER models to analyze the performance of them.

B. Integration-based Optimal Receiver

The integration-based optimal receiver relies on noncoherent detection. Let T_0 denote the period of the carrier signals, i.e., $T_0 = 2\pi/\omega_0$. For a bit “0”, the output of the integrator is

$$h_{int,0} = \int_0^{T_0} |v_{r0}(t)| dt \quad (3)$$

$$= \frac{r_l c_1 i_{sw}}{\omega_0} \left(1 - e^{-\frac{2\pi}{\alpha Q_t}} \right). \quad (4)$$

Since the received voltage $h_{int,0}$ is around 0, to better distinguish the bit “1” and bit “0”, a full-wave bridge rectifier can be used to ensure the received voltage for bit “1” is always larger than 0. Thus, for a bit “1”, the output of the integrator is

$$h_{int,1} = \int_0^{T_0/2} -v_{r1}(t) dt + \int_{T_0/2}^{T_0} v_{r1}(t) dt \quad (5)$$

$$= \frac{4r_l c_1 c_2}{\omega_0} + \frac{4Q_t^2 r_l c_1}{(4Q_t^2 + 1)\omega_0} (i_{sw} - c_2) (1 + e^{-\frac{\pi}{Q_t}} + 2e^{-\frac{2\pi}{Q_t}}). \quad (6)$$

To reduce the BER, we need to maximize $|h_{int,0} - h_{int,1}|$. Note that, when Q_t is small, the coupling between the transmitter and the receiver is weak; the signal-to-noise ratio (SNR) can be very small. Thus, it is challenging to detect bit

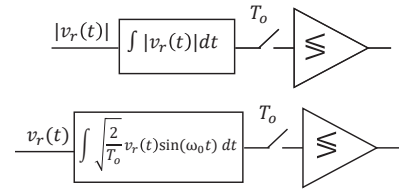


Fig. 3. Receiver architecture: the integration-based optimal receiver (upper) and the correlation-based optimal receiver (lower).

“1” and bit “0”. When Q_t is large, we have the following approximations

$$h_{int,1} \approx \frac{4i_{sw}r_l c_1}{\omega_0} \quad (7)$$

$$h_{int,0} \approx \frac{2\pi i_{sw}r_l c_1}{\omega_0 \alpha Q_t}. \quad (8)$$

When switching at the maximum current, i_{sw} can be approximated by $c_2/2$. In this case, $|h_{int,0} - h_{int,1}| = |(4 - \frac{2\pi}{\alpha Q_t}) \frac{i_{sw}r_l c_1}{\omega_0}|$. To increase $|h_{int,0} - h_{int,1}|$, we can increase Q_t , c_1 , and i_{sw} . Since c_1 and i_{sw} are determined by the communication distance and transmission power, respectively, usually, they cannot be changed. Increasing the coil quality factor is an effective solution.

Assume that $N_0/2$ is the noise power spectral density. Then, the noise variance is

$$\mathbb{E} \left[\int_0^{T_0} z(t) dt \int_0^{T_0} z^*(\tau) d\tau \right] \quad (9)$$

$$= \int_0^{T_0} \int_0^{T_0} \mathbb{E}[z(t)z^*(\tau)] dt d\tau = \int_0^{T_0} \frac{N_0}{2} d\tau = \frac{N_0 T_0}{2}. \quad (10)$$

where $(\cdot)^*$ is the complex conjugate and $\mathbb{E}(\cdot)$ is the expectation. As we can see, the noise power spectral density depends on the sampling interval and we need to scale it by T_0 . The BER can be given as [8]

$$P_{e,int} = \mathcal{Q} \left(\frac{|h_{int,0} - h_{int,1}|}{\sqrt{2N_0 T_0}} \right) \approx \mathcal{Q} \left(\frac{\frac{4\alpha Q_t - 2\pi}{\alpha Q_t} i_{sw} r_l c_1 \sqrt{T_0}}{\sqrt{8\pi^2 N_0}} \right) \quad (11)$$

where $\mathcal{Q}(\cdot)$ is the Q-function. The optimal detection threshold is $v_{int} = (h_{int,1} - h_{int,0})/2$, which can minimize the BER.

C. Correlation-based Optimal Receiver

The second optimal receiver is based on coherent detection. The $\sqrt{\frac{2}{T_0}} \sin(\omega_0 t)$ for $0 \leq t \leq T_0$ can be used as an orthonormal basis for On-Off keying. Thus, the optimal matched filter is $\sqrt{\frac{2}{T_0}} \sin(\omega_0(T_0 - t))$ for $0 \leq t \leq T_0$. The received signal can be correlated with this filter and then sampled every T_0 . For a bit “1”, the sampled output is

$$h_{cor,1} = \sqrt{\frac{2}{T_0}} \int_0^{T_0} v_{r1}(t) \sin(\omega_0(T_0 - t)) dt = r_l c_1 c_2 \sqrt{\frac{T_0}{2}} - \frac{r_l c_1}{\sqrt{2T_0}} (i_{sw} - c_2) (e^{-\frac{\pi}{Q_t}} - 1) \left[\frac{2Q_t}{\omega_0} - \frac{1}{\frac{\omega_0}{2Q_t} + 8\omega_0 Q_t} \right] \quad (12)$$

For a bit “0”, the sampled output is

$$h_{cor,0} = \sqrt{\frac{2}{T_0}} \int_0^{T_0} v_{r0}(t) \sin(\omega_0(T_0 - t)) dt \quad (13)$$

$$= \sqrt{\frac{2}{T_0}} \frac{r_l c_1 i_{sw}}{\alpha Q_t \omega_0 + \frac{\omega_0}{\alpha Q_t}} \left(e^{-\frac{2\pi}{\alpha Q_t}} - 1 \right). \quad (14)$$

Similarly, when Q_0 is small, both $h_{cor,1}$ and $h_{cor,0}$ are approximately 0 since the coupling between coils are weak and c_1 is small. When Q_t is large, we can obtain

$$h_{cor,1} \approx \sqrt{\frac{T_0}{2}} r_l c_1 i_{sw}; \quad h_{cor,0} \approx 0. \quad (15)$$

Therefore, the approximated BER can be written as

$$P_{e,cor} \approx \mathcal{Q} \left(\frac{|h_{cor,0} - h_{cor,1}|}{\sqrt{2N_0}} \right) \approx \mathcal{Q} \left(\sqrt{\frac{T_0 r_l^2 c_1^2 i_{sw}^2}{4N_0}} \right). \quad (16)$$

To minimize the BER, it is desirable to increase the transmission power, which increases i_{sw} , or increase the mutual coupling between coils, which increases c_1 . Similarly, the optimal detection threshold is $v_{cor} = (h_{cor,1} - h_{cor,0})/2$.

III. SIMULATION AND NUMERICAL ANALYSIS

In this section, we numerically evaluate the BER performance of the proposed receiving architectures. Also, we perform simulations to verify the performance. The effect of Q_t is shown in Fig. 4. The carrier frequency is 13.56 MHz. The resistances r_s , r_l , r_{l1} , and r_{l2} are all set as 1Ω . The switching current $i_{sw} = c_2/2$ and $v_0 = 0.1$ V. $N_0 = -90$ dBm/Hz and $m = 0.05Q_t/\omega_0$. Then, we gradually increase Q_t starting from 1. From Fig. 4, we have the following three observations. First, the approximated models under the assumption of large Q_t can closely track the exact models for both the integration-based optimal receiver and the correlation-based optimal receiver. Second, as Q_t increases the BER of both the integration-based optimal receiver and the correlation-based optimal receiver monotonically decreases, which indicates that a large Q_t can efficiently reduce BER. Third, as Q_t increases the gain of using correlation-based optimal receiver over that of using integration-based optimal receiver increases from 0 to around 20 dB.

To further analyze the effect of the SNR, we use $T_0 c_1^2 i_{sw}^2 / N_0$ as an indicator. Note that i_{sw}^2 is proportional to the transmission power and c_1^2 is proportional to the channel response. As a result, $c_1^2 i_{sw}^2$ is proportional to the receiver power for one bit and multiplying by the symbol time T_0 we can obtain the bit/symbol energy. We use the approximated BER model to evaluate the performance of the two receivers. As shown in Fig. 5, the correlation-based optimal receiver has a gain of 20 dB in the high-SNR regime. In the low-SNR regime, the two receivers have similar performance.

IV. CONCLUSION

Magnetic induction (MI) communication receives wide acceptance in extreme environments. It uses lower MHz or kHz carrier signals and high quality factor coils, which significantly limits its signal bandwidth. Direct antenna modulation (DAM)

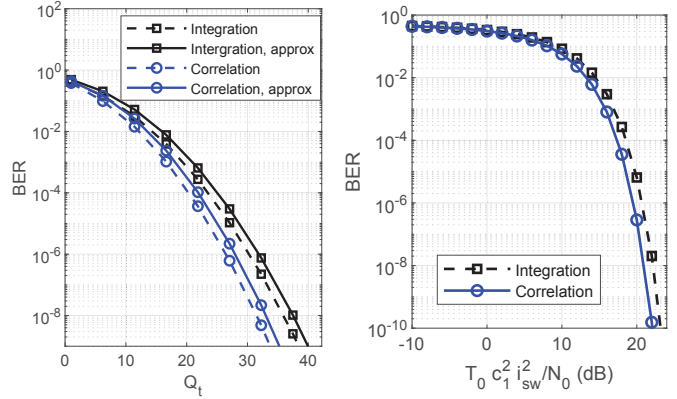


Fig. 4. Effect of coil quality factor.

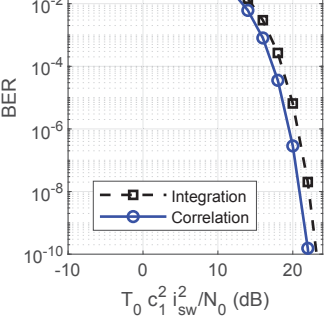


Fig. 5. Effect of signal-to-noise ratio.

efficiently overcome this issue by modulating signals in the antenna. In this paper, we propose two receiving architectures using integration-based and correlation-based solutions. We analytically derive and optimize the receivers and numerically evaluate and compare their performance. The results show that the correlation-based solution achieves lower bit-error-rate (BER) but it requires coherent detection. While the integration-based solution has higher BER, it uses noncoherent detection, which is simple and low-cost. Our future work will implement the proposed receivers and develop a complete DAM-based MI communication system.

ACKNOWLEDGMENT

This material is based upon work supported by the National Science Foundation under Grant No. HRD1953460. Any opinions, findings, and conclusions or recommendations expressed in this material are those of the authors and do not necessarily reflect the views of the National Science Foundation. This work is also supported in part by The Thomas F. and Kate Miller Jeffress Memorial Trust, Bank of America, Trustee.

REFERENCES

- [1] X. Dong, M. C. Vuran, and S. Irmak, “Autonomous precision agriculture through integration of wireless underground sensor networks with center pivot irrigation systems,” *Ad Hoc Networks*, vol. 11, no. 7, pp. 1975–1987, 2013.
- [2] Z. Sun, P. Wang, M. C. Vuran, M. A. Al-Rodhaan, A. M. Al-Dhelaan, and I. F. Akyildiz, “Mise-pipe: Magnetic induction-based wireless sensor networks for underground pipeline monitoring,” *Ad Hoc Networks*, vol. 9, no. 3, pp. 218–227, 2011.
- [3] S. Kisseleff, I. F. Akyildiz, and W. H. Gerstacker, “Throughput of the magnetic induction based wireless underground sensor networks: Key optimization techniques,” *IEEE Transactions on Communications*, vol. 62, no. 12, pp. 4426–4439, 2014.
- [4] H. Guo and K. D. Song, “Reliable through-metal wireless communication using magnetic induction,” *IEEE Access*, vol. 7, pp. 115 428–115 439, 2019.
- [5] N. Saeed, M.-S. Alouini, and T. Y. Al-Naffouri, “Toward the internet of underground things: A systematic survey,” *IEEE Communications Surveys & Tutorials*, vol. 21, no. 4, pp. 3443–3466, 2019.
- [6] U. Azad and Y. E. Wang, “Direct antenna modulation (dam) for enhanced capacity performance of near-field communication (nfc) link,” *IEEE Transactions on Circuits and Systems I: Regular Papers*, vol. 61, no. 3, pp. 902–910, 2013.
- [7] R. Zhu and Y. E. Wang, “A modified qpsk modulation technique for direct antenna modulation (dam) systems,” in *2014 IEEE Antennas and Propagation Society International Symposium (APSURSI)*. IEEE, 2014, pp. 1592–1593.
- [8] J. G. Proakis and M. Salehi, *Digital Communication 5th Edition*. McGraw Hill, 2007.